

See discussions, stats, and author profiles for this publication at: <https://www.researchgate.net/publication/275025184>

# A New Strategy To Synthesize Temperature-and pH-Sensitive Multicompartment Block Copolymer Nanoparticles by Two Macro-RAFT Agents Comediated Dispersion Polymerization

ARTICLE *in* MACROMOLECULES · OCTOBER 2014

Impact Factor: 5.8 · DOI: 10.1021/ma501598k

---

CITATIONS

8

READS

57

## 6 AUTHORS, INCLUDING:



Pengfei Shi

Nankai University

9 PUBLICATIONS 49 CITATIONS

[SEE PROFILE](#)



Quanlong Li

Nankai University

14 PUBLICATIONS 117 CITATIONS

[SEE PROFILE](#)



Shentong Li

Nankai University

17 PUBLICATIONS 166 CITATIONS

[SEE PROFILE](#)



Wangqing Zhang

Nankai University

105 PUBLICATIONS 2,221 CITATIONS

[SEE PROFILE](#)

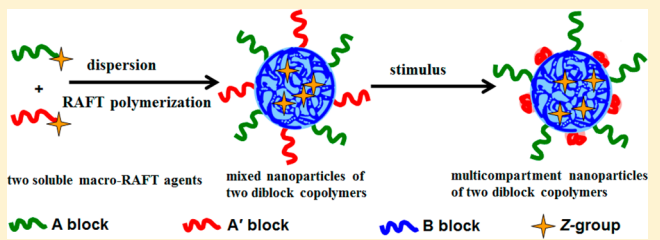
## A New Strategy To Synthesize Temperature- and pH-Sensitive Multicompartment Block Copolymer Nanoparticles by Two Macro-RAFT Agents Comediated Dispersion Polymerization

Pengfei Shi, Quanlong Li, Xin He, Shentong Li, Pingchuan Sun, and Wangqing Zhang\*

Key Laboratory of Functional Polymer Materials of the Ministry of Education, Collaborative Innovation Center of Chemical Science and Engineering (Tianjin), Institute of Polymer Chemistry, Nankai University, Tianjin 300071, China

### Supporting Information

**ABSTRACT:** Multicompartment block copolymer nanoparticles (MCBNs) arouse great interest due to their special structure and wide application. However, synthesis of MCBNs suffers from great inconvenience and difficulty. In this contribution, an efficient strategy to prepare well-defined temperature- and pH-sensitive MCBNs constructed with two diblock copolymers of poly(4-vinylpyridine)-*b*-polystyrene (P4VP-*b*-PS) and poly(*N*-isopropylacrylamide)-*b*-polystyrene (PNIPAM-*b*-PS) through the two macro-RAFT agents comediated dispersion polymerization is proposed. In this two macro-RAFT agents comediated dispersion polymerization, two macro-RAFT agents having similar polymerization degree are simultaneously adopted, and onset micellization of PNIPAM-*b*-PS and P4VP-*b*-PS occurs simultaneously to form mixed corona–core nanoparticles containing a PNIPAM/P4VP mixed corona and a PS core. In neutral water at room temperature, the corona-forming P4VP block deposits on the PS core to form MCBNs, which contain a solvophobic PS core, discrete P4VP nodules on the PS core, and a solvophilic PNIPAM corona. The parameters affecting the MCBNs structure are investigated. It is found that the higher percent of the poly(4-vinylpyridine) trithiocarbonate (P4VP-TTC) macro-RAFT agent and the shorter PS block, the larger the size of the P4VP nodules on MCBNs. The synthesized MCBNs are temperature- and pH-responsive. Through the phase transition of the temperature-responsive PNIPAM block and the pH-responsive P4VP block, the morphology of MCBNs can be changed. Our strategy of the two macro-RAFT agents comediated dispersion polymerization is believed sufficiently to overcome the inconvenience and difficulty in synthesis of well-defined MCBNs.



### 1. INTRODUCTION

Of all the self-assemblies of block copolymers, multicompartment block copolymer nanoparticles (MCBNs) composed of a solvophilic corona and a solvophobic microphase-separated core have garnered great interest,<sup>1–3</sup> since the microphase-separated core in MCBNs presents the opportunity to selectively entrap and release multiple hydrophobic ingredients with enhancement in functionality over simple corona–core structures containing a single hydrophobic environment.<sup>4</sup> Because of the special structure, MCBNs are expected to have promising applications in scheduled delivery of multi-drugs, selective catalysis, and nanotechnology.<sup>1–3</sup> However, synthesis of well-controlled MCBNs suffers from great inconvenience and difficulty.

Up to now, two strategies are proposed to prepare MCBNs. The first strategy is through micellization of linear ABC triblock terpolymers,<sup>5–25</sup> ABC miktoarm star terpolymers,<sup>26–35</sup> and ABCA and ABCBA multiblock copolymers,<sup>36–40</sup> in which A represents the solvophilic block and B and C represent two incompatible solvophobic blocks throughout this article, in the selective solvent for the A block. Through proper choice of the polymer architecture and the processing conditions, a wide diversity of MCBNs including cylinders, segmented worms,

disks, plates, toroids, and raspberry-like nanoparticles have been prepared.<sup>5–40</sup> In this subject, notable contributions have been made by the research groups led by Müller,<sup>21–26</sup> Hillmyer,<sup>27–31</sup> Laschewsky,<sup>12–14</sup> Wooley,<sup>15–18</sup> Liu,<sup>19,20</sup> and Gohy.<sup>39,40</sup> However, this strategy suffers from the disadvantages of the complex polymer structure such as fluorinated block terpolymers or miktoarm star terpolymers and the diluted polymer concentration usually below 1%. Generally, synthesis of these complex block copolymers is a laborious work and therefore limits its potential application.

The second strategy to prepare MCBNs is through the comicellization or blending of two or more presynthesized block copolymers in a suitable block-selective solvent.<sup>41–54</sup> For example, Lodge and co-workers have used blends of AB diblock copolymer and ABC miktoarm star terpolymer,<sup>46</sup> and Pochan and co-workers have used blends of AB and BC diblock copolymers to tune the morphology of MCBNs.<sup>47–49</sup> Besides, Srinivas and Pitera suggested that a binary mixture of two different diblock copolymers with a common hydrophobic

Received: August 30, 2014

Revised: October 9, 2014

Published: October 21, 2014

Table 1. Experimental Details and Summary of the Synthesized Macro-RAFT Agents

entry	macro-RAFT	$[M]_0:[CTA]_0:[I]_0$	time (h)	conv <sup>a</sup> (%)	M <sub>n</sub> (kg/mol)			PDI <sup>e</sup>
					M <sub>n,th</sub> <sup>b</sup>	M <sub>n,GPC</sub> <sup>c</sup>	M <sub>n,NMR</sub> <sup>d</sup>	
A1	P4VP <sub>114</sub> -TTC	800:4:1	12	57	12.4	10.7	12.5	1.03
A2	P4VP <sub>146</sub> -TTC	1000:4:1	12	58	15.7	14.6	15.9	1.03
B1	PNIPAM <sub>98</sub> -TTC	480:4:1	2	82	11.5	11.8	12.9	1.02
B2	PNIPAM <sub>137</sub> -TTC	640:4:1	2	86	15.9	16.9	17.3	1.02

<sup>a</sup>The monomer conversion determined by <sup>1</sup>H NMR analysis. <sup>b</sup>Theoretical molecular weight determined by monomer conversion. <sup>c</sup>The molecular weight determined by GPC analysis. <sup>d</sup>The molecular weight determined by <sup>1</sup>H NMR analysis. <sup>e</sup>The PDI ( $M_w/M_n$ ) value determined by GPC analysis.

block but sufficiently dissimilar hydrophilic blocks reliably self-assembles into patchy micelles in water through the phase separation of the two hydrophilic blocks on the surface of the mixed micelles.<sup>50</sup> This comicellization or blending strategy has the advantages of the convenient synthesis of diblock copolymer compared with the ABC or BAC triblock terpolymers and the tunable structure of MCBNs by changing the ratio of the diblock copolymers in the blended polymers.<sup>41–45</sup> However, besides the targeted mixed micelles constructed with two different block copolymers, nonergodic micelles, which are composed of just one block copolymer either of AB or BC, usually form in the comicellization or blending strategy.<sup>55</sup> Besides, since the micelle exchange dynamics is generally very slow due to the high polymer molecular weight,<sup>56,57</sup> translating nonergodic micelles into mixed micelles by intermicelle macromolecular exchange is very difficult.

In the previous communication,<sup>58</sup> a new and efficient strategy to synthesize MCBNs constructed with two diblock copolymers through the two macro-RAFT agent comediated dispersion polymerization is proposed. This strategy includes (1) *in situ* synthesis of mixed corona–core nanoparticles of the AB and A'B diblock copolymers through the two macro-RAFT agents comediated dispersion polymerization and (2) deposition of the corona-forming A' block on the core of the B block to form MCBNs, which contain a solvophobic core of the B block, discrete nodules of the A' block on the B core, and a solvophilic corona of the A block. This two macro-RAFT agents comediated dispersion polymerization is dominated to be a valid method of *in situ* synthesis of mixed nanoparticles or MCBNs constructed with two diblock copolymers with polymer concentration as high as those in the general macro-RAFT agent mediated dispersion polymerization.<sup>59,60</sup>

In this contribution, we extend this strategy to prepare temperature- and pH-sensitive MCBNs constructed with two diblock copolymers of poly(*N*-isopropylacrylamide)-*b*-polystyrene (PNIPAM-*b*-PS) and poly(4-vinylpyridine)-*b*-polystyrene (P4VP-*b*-PS). The synthesized MCBNs dispersed in water contain a solvophobic core of the polystyrene (PS) block, several discrete nanosized nodules of the poly(4-vinylpyridine) (P4VP) block on the PS core, and a solvophilic corona of the poly(*N*-isopropylacrylamide) (PNIPAM) block. The structure evolution of the MCBNs with monomer conversion during the dispersion RAFT polymerization is investigated, and the parameters affecting the structure of MCBNs are clarified. The synthesized MCBNs are both temperature- and pH-sensitive, and their morphology can be changed by either pH or temperature jump.

## 2. EXPERIMENTAL SECTION

**2.1. Materials.** The monomer of *N*-isopropylacrylamide (NIPAM, >99%, Acros Organics) was purified by recrystallization in the acetone/*n*-hexane mixture (50:50 by volume). The monomers of 4-vinylpyridine (4VP, 96%, Alfa) and styrene (St, >98%, Tianjin Chemical Company) were distilled under reduced pressure prior to use. S-1-Dodecyl-S'-( $\alpha,\alpha'$ -dimethyl- $\alpha'$ -acetic acid) trithiocarbonate (DDMAT) was synthesized as discussed elsewhere.<sup>61</sup> The initiator of 2,2'-azobis(2-methylpropionitrile) (AIBN, >99%, Tianjin Chemical Company) was purified by recrystallization from ethanol. All the other chemical reagents were analytic grade and used as received. Deionized water was used in the present study.

**2.2. Synthesis of the Macro-RAFT Agents.** Two macro-RAFT agents, poly(*N*-isopropylacrylamide) trithiocarbonate (PNIPAM-TTC) and poly(4-vinylpyridine) trithiocarbonate (P4VP-TTC) in which TTC represents the RAFT terminal of trithiocarbonate, were synthesized by solution RAFT polymerization using AIBN as initiator and DDMAT as RAFT agent.

In the synthesis of the PNIPAM-TTC macro-RAFT agent, the monomer of NIPAM [7.50 g (0.0663 mol) or 10.00 g (0.0884 mol)], DDMAT (202.0 mg, 0.554 mmol), and AIBN (22.6 mg, 0.138 mmol) dissolved in 1,4-dioxane (30.0 g) were added into a 50 mL Schlenk flask with a magnetic bar. The solution was degassed with nitrogen at 0 °C, and then the flask content was immersed into preheated oil bath at 70 °C for 2 h. The polymerization was quenched by rapid cooling upon immersion of the flask in iced water. The monomer conversion was determined by <sup>1</sup>H NMR analysis. The synthesized polymer was precipitated into diethyl ether at 0 °C, collected by three precipitation/filtration cycles, and then dried at room temperature under vacuum. Two PNIPAM-TTC macro-RAFT agents, PNIPAM<sub>98</sub>-TTC and PNIPAM<sub>137</sub>-TTC, with different polymerization degree (DP) at 98 and 137 were prepared by keeping the molar ratio of  $[NIPAM]_0:[DDMAT]_0:[AIBN]_0$  at 480:4:1 and 600:4:1, respectively.

The P4VP-TTC macro-RAFT agents, P4VP<sub>114</sub>-TTC and P4VP<sub>146</sub>-TTC, were prepared by RAFT polymerization under  $[4VP]_0:[DDMAT]_0:[AIBN]_0$  at 800:4:1 and 1000:4:1 at 70 °C for 12 h. The monomer conversion was determined by <sup>1</sup>H NMR analysis. The P4VP-TTC macro-RAFT agent was precipitated into diethyl ether and then dried at room temperature under vacuum. The synthesis details are shown in Table 1.

**2.3. Two Macro-RAFT Agents Comediated Dispersion Polymerization and Synthesis of MCBNs.** The two macro-RAFT agents comediated dispersion polymerization of styrene in the ethanol/water mixture (80/20 by weight) was performed at 70 °C under  $[St]_0:[PNIPAM-TTC + P4VP-TTC]_0:[AIBN]_0 = 1800:6:2$  and with the weight percent of the fed monomer plus the two macro-RAFT agents at 15%. Herein, a typical dispersion RAFT polymerization under  $[St]_0:[PNIPAM-TTC]_0:[P4VP-TTC]_0:[AIBN]_0 = 1800:3:3:2$  is introduced. Into a 25 mL Schlenk flask with a magnetic bar, PNIPAM<sub>137</sub>-TTC (0.126 g, 0.0079 mmol), P4VP<sub>146</sub>-TTC (0.127 g, 0.0081 mmol), St (0.500 g, 4.80 mmol), and the initiator of AIBN (0.876 mg, 0.0053 mmol) dissolved in the ethanol/water mixture (4.00 g, 80/20 by weight) were added. The flask content was vigorously stirred for 5 min and degassed with nitrogen at 0 °C, and then the polymerization was initiated by immersing the flask into preheated oil bath at 70 °C. After a given time, the polymerization was

Scheme 1. Schematic Synthesis of MCBNs Constructed with Two Diblock Copolymers

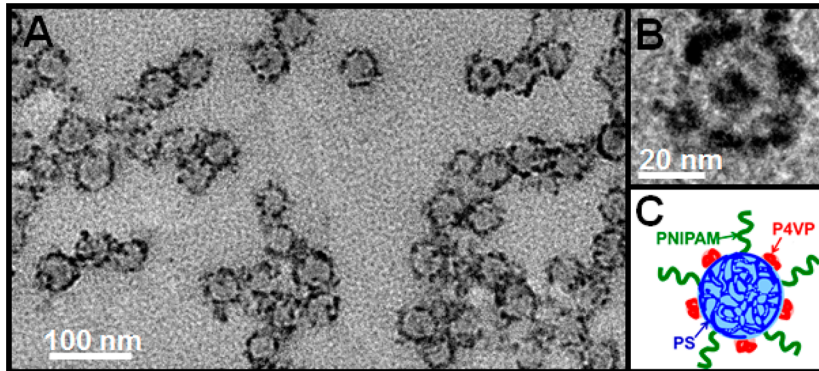
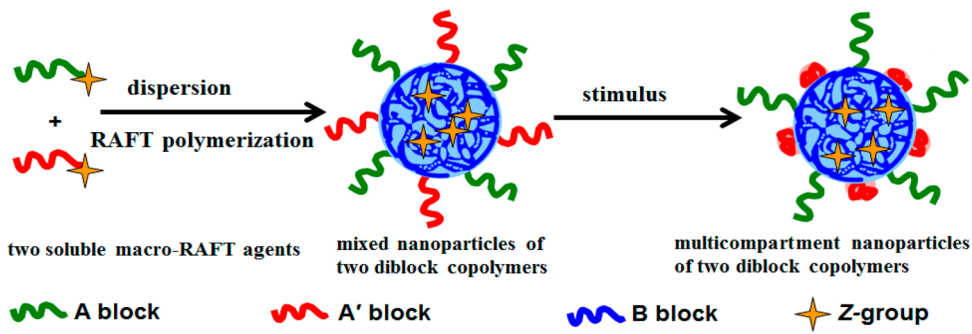


**Figure 1.** TEM images (A, B) and the schematic structure (C) of the typical MCBNs prepared through the two macro-RAFT agents comediated dispersion polymerization. Polymerization conditions: St (0.500 g, 4.80 mmol), the ethanol/water mixture (4.00 g, 80/20 by weight),  $[St]_0:[PNIPAM_{137}\text{-TTC}]_0:[P4VP_{146}\text{-TTC}]_0:[AIBN]_0 = 1800:2:4:2$ , 70 °C, 14 h.

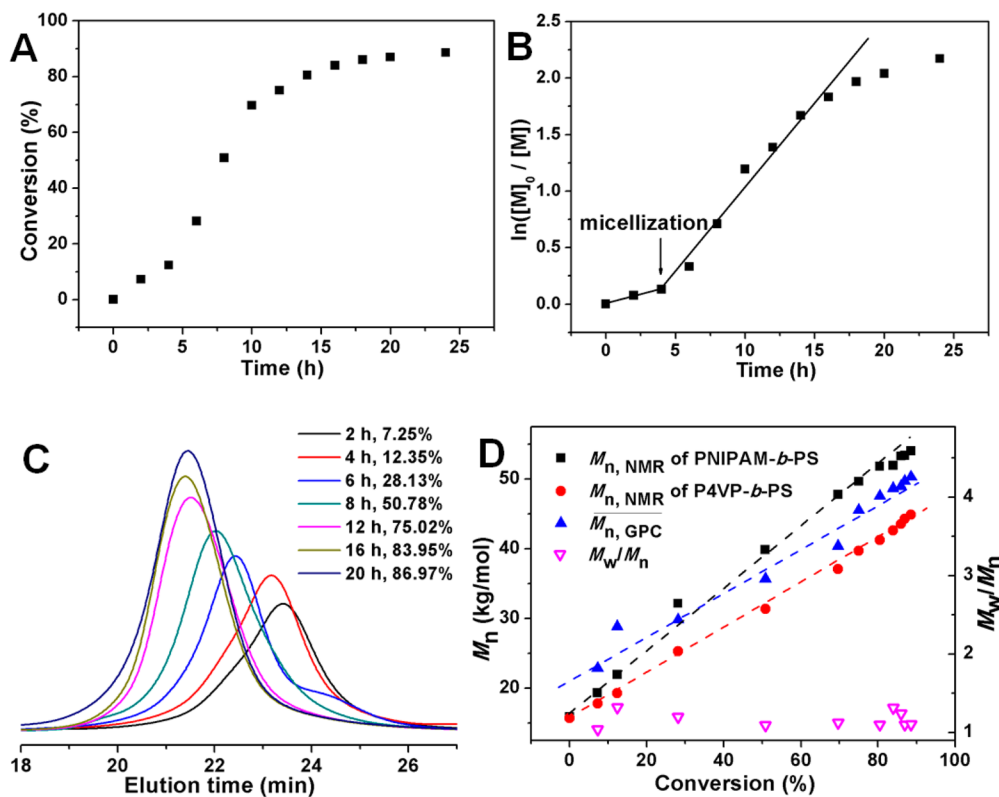


**Figure 2.** Monomer conversion–time plot (A) and the  $\ln([M]_0/[M])$ –time plot (B) for the two macro-RAFT agents comediated dispersion polymerization, the GPC traces (C), and the average molecular weight  $M_n$ ,<sub>GPC</sub> and PDI of the PNIPAM-*b*-PS/P4VP-*b*-PS mixture and  $M_n$ ,<sub>NMR</sub> of the separated diblock copolymers of PNIPAM-*b*-PS and P4VP-*b*-PS (D). Polymerization conditions: St (0.500 g, 4.80 mmol), the ethanol/water mixture (4.00 g, 80/20 by weight),  $[St]_0:[PNIPAM_{137}\text{-TTC}]_0:[P4VP_{146}\text{-TTC}]_0:[AIBN]_0 = 1800:3:3:2$ , 70 °C.

quenched by immersing the flask in iced water, and the monomer conversion was detected by UV-vis analysis as discussed elsewhere.<sup>62</sup> The *in situ* synthesized dispersion of the diblock copolymer nano-objects was dialyzed initially against ethanol for 2 days to remove the residual St monomer and then against water at room temperature (20–25 °C) for 3 days to remove ethanol (molecular weight cutoff: 7000 Da) to afford the aqueous dispersion of MCBNs. The removal of St was judged by the UV-vis analysis of the dialysis solution at 245 nm.

**2.4. Collection and Separation of the PNIPAM-*b*-PS/P4VP-*b*-PS Mixture.** To collect the PNIPAM-*b*-PS/P4VP-*b*-PS mixture for gel permeation chromatography (GPC) analysis and <sup>1</sup>H NMR analysis, the aqueous dispersion of MCBNs was extracted with dichloromethane (20 mL × 2). The organic phase was collected and dried over anhydrous magnesium sulfate. After filtration of magnesium sulfate and removal of the solvent, the polymer was collected and dried under vacuum at room temperature overnight to afford the PNIPAM-*b*-PS/P4VP-*b*-PS mixture in pale yellow.

To separate PNIPAM-*b*-PS or P4VP-*b*-PS from the PNIPAM-*b*-PS/P4VP-*b*-PS mixture, the PNIPAM-*b*-PS/P4VP-*b*-PS mixture (0.3–0.8 g) was dispersed in acetone (2 mL) at room temperature, magnetically stirred for 1 h, and then separated by centrifugation (12 500 rpm, 30 min). The supernatant solution was collected, and the solvent of acetone was removed by rotary evaporation under reduced pressure at 30 °C to afford the PNIPAM-*b*-PS diblock copolymer. The precipitate was collected, dispersed in acetone (10 mL), magnetically stirred for 1 h, and then separated by centrifugation (12 500 rpm, 30 min). The supernatant solution was discarded, and the precipitate was collected. The collected precipitate was washed with acetone (5 mL × 4) and then dried under vacuum at room temperature to afford the P4VP-*b*-PS diblock copolymer. Note: the separation of the diblock copolymer mixture is somewhat different depending on the DP of the PS block, and 2 or 3 dispersion/washing cycles may be needed. The separation of the PNIPAM-*b*-PS/P4VP-*b*-PS mixture was judged by <sup>1</sup>H NMR analysis of the separated diblock copolymer.

**2.5. Characterization.** The <sup>1</sup>H NMR analysis was performed on a Bruker Avance III 400 MHz NMR spectrometer using CDCl<sub>3</sub> as solvent. The GPC analysis was detected using a Viscotek GPC Max Ve2001 solvent/sample module equipped with a DAWN HELEOS 8 light scattering photometer, a ViscoStar viscometer, and an Optilab rEX interferometric refractometer and with three Mz-Gel SD plus 10 μm columns, in which DMF was used as eluent at flow rate of 1.0 mL/min at 25 °C and the narrow-polydispersity polystyrene was used as calibration standard. The phase-transition temperature (PTT) of the thermoresponsive polymer was determined by turbidity measurement at 500 nm on a Varian 100 UV-vis spectrophotometer equipped with a thermoregulator (±0.1 °C) with the heating/cooling rate at 1 °C/min. The PTT values were determined at the middle point of the transmittance change. Dynamic light scattering (DLS) analysis was performed on Nano-ZS90 (Malvern) laser light scattering spectrometer with He-Ne laser at the wavelength of 633 nm at 90° angle, in which the apparent hydrodynamic diameter D<sub>h</sub><sup>app</sup> of MCBNs with the diluted polymer concentration was determined by intensity following the CONTIN method. TEM observation was performed using a Tecnai G2 F20 electron microscope at an acceleration of 200 kV. To detect the colloidal morphology, a small drop of the diluted dispersion of MCBNs was deposited onto a piece of copper grid, dried at room temperature, negatively stained with 1.5 wt % aqueous solution of phosphotungstic acid, and then stained with I<sub>2</sub> vapor at 50 °C for 30 min under reduced pressure, and last observed by TEM.

### 3. RESULTS AND DISCUSSION

**3.1. Synthesis of the PNIPAM-TTC and P4VP-TTC Macro-RAFT Agents.** The macro-RAFT agents of PNIPAM-TTC and P4VP-TTC were synthesized by the solution RAFT polymerization using DDMAT as RAFT agent and AIBN as initiator. By varying the molar ratio of the fed monomer/DDMAT and the polymerization time, two P4VP-based macro-RAFT agents of P4VP<sub>114</sub>-TTC and P4VP<sub>146</sub>-TTC and two

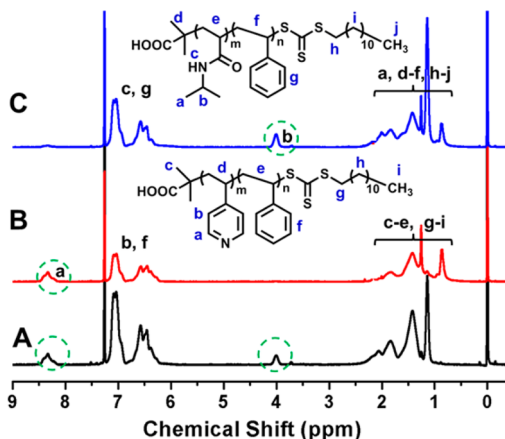


**Figure 3.** <sup>1</sup>H NMR spectra of the PNIPAM-*b*-PS/P4VP-*b*-PS mixture prepared at the polymerization time of 16 h (A) and the separated diblock copolymers of P4VP-*b*-PS (B) and PNIPAM-*b*-PS (C).

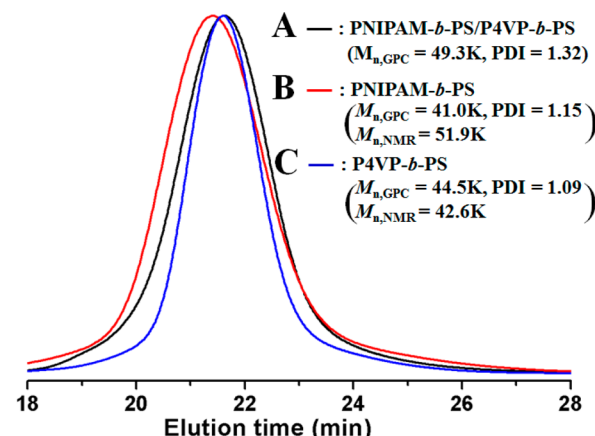


**Figure 4.** GPC traces of the PNIPAM-*b*-PS/P4VP-*b*-PS mixture prepared at the polymerization time of 16 h (A) and the separated PNIPAM-*b*-PS (B) and P4VP-*b*-PS (C).

PNIPAM-based macro-RAFT agents of PNIPAM<sub>98</sub>-TTC and PNIPAM<sub>137</sub>-TTC were prepared. The four macro-RAFT agents were characterized by GPC analysis (Figure S1) and <sup>1</sup>H NMR analysis (Figure S2), and the results are summarized in Table 1. The four macro-RAFT agents have satisfied low PDI values, and the theoretical molecular weight M<sub>n,th</sub> calculated by monomer conversion,<sup>63</sup> the molecular weight M<sub>n,GPC</sub> by GPC analysis, and the molecular weight M<sub>n,NMR</sub> by <sup>1</sup>H NMR analysis, which is calculated by comparing the integration area of the RAFT terminal to those in the polymer backbone, are similar to each other, suggesting the good control in the solution RAFT polymerization.

**3.2. Outline of Synthesis of MCBNs.** Different from the general macro-RAFT agent mediated dispersion polymerization,<sup>64–70</sup> two different macro-RAFT agents, PNIPAM<sub>137</sub>-TTC and P4VP<sub>146</sub>-TTC, are simultaneously used in the present two macro-RAFT agents comediated dispersion polymerization, as shown in Scheme 1. These two macro-RAFT agents comediated dispersion polymerization leads to the simultaneous formation of the two diblock copolymers of PNIPAM-*b*-PS and P4VP-*b*-PS in the polymerization medium of the 80/20 ethanol/water mixture. The solvent of the 80/20 ethanol/water mixture is chosen because it is a good solvent for the two macro-RAFT agents of P4VP<sub>146</sub>-TTC and PNIPAM<sub>137</sub>-TTC

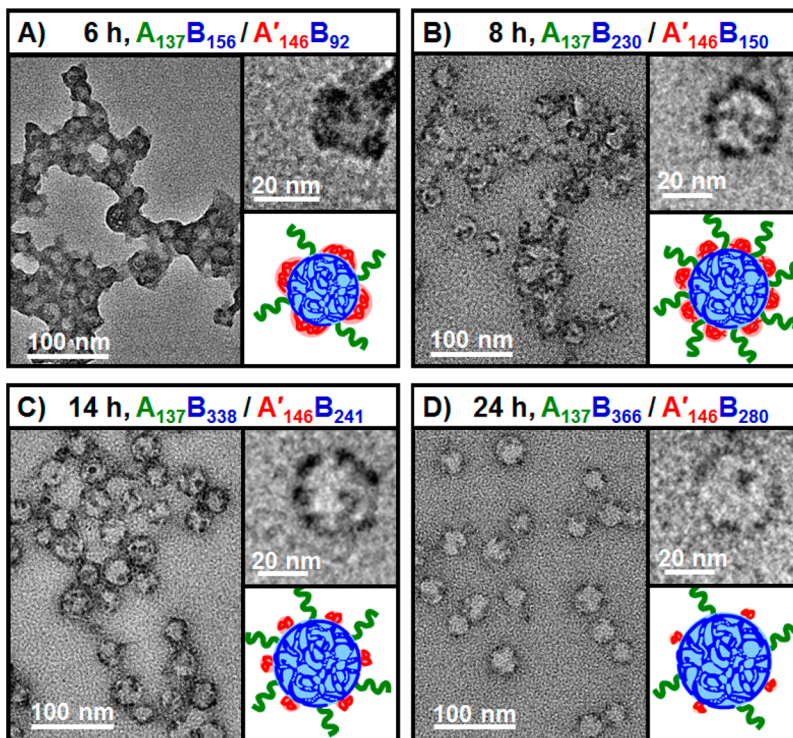


**Figure 5.** TEM images of the MCBNs prepared through the two macro-RAFT agents comediated dispersion polymerization at the polymerization time of 6 (A), 8 (B), 14 (C), and 24 h (D). Insets: the schematic structure of MCBNs.

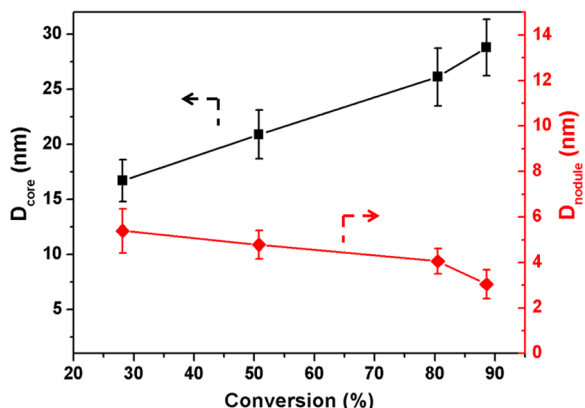


**Figure 6.** Monomer conversion dependent  $D_{\text{core}}$  of the PS core and  $D_{\text{nodule}}$  of the P4VP nodules in MCBNs.

but a nonsolvent for the PS block in the synthesized diblock copolymers of PNIPAM-*b*-PS and P4VP-*b*-PS, which is essential for the polymerization-induced self-assembly. With the extension of the PS block, the DP of the PS block ( $D_P$ ) increases gradually, and the self-assembly of PNIPAM-*b*-PS and P4VP-*b*-PS occurs when  $D_P$  approaches to a critical point.

To form mixed nanoparticles of two diblock copolymers but not nonergodic nanoparticles constructed with one diblock copolymer in the two macro-RAFT agents comediated dispersion polymerization, two requisites listed below are essential. First, the simultaneous onset micellization of PNIPAM-*b*-PS and P4VP-*b*-PS is needed. Previous results demonstrated that the functional RAFT group and the DP of the macro-RAFT agent exert great influence on the polymerization kinetics,<sup>70,71</sup> and therefore the two P4VP<sub>146</sub>-TTC and PNIPAM<sub>137</sub>-TTC macro-RAFT agents having the same RAFT terminal and having similar DP are specially designed. The

polymerization kinetics shown in Figure S3 shows the almost simultaneous onset micellization of PNIPAM-*b*-PS and P4VP-*b*-PS in the two cases of the individual macro-RAFT agent mediated dispersion polymerization, although the PNIPAM<sub>137</sub>-TTC macro-RAFT agent mediated dispersion polymerization runs slightly faster. Second, fast micelle exchange dynamics is available in the initial RAFT polymerization. For two small surfactants, the micelle exchange dynamics between surfactant micelles is fast, and therefore mixed micelles are usually formed in aqueous surfactant solution.<sup>46,72</sup> For amphiphilic block copolymer micelles, due to the high molar mass of polymer, the polymer chains are usually frozen in the solvent, and therefore the exchange dynamics between block copolymer micelles is very slow.<sup>46–49,54,55,72</sup> In the present two macro-RAFT agents comediated dispersion polymerization typically under  $[St]_0$ : [PNIPAM<sub>137</sub>-TTC]<sub>0</sub>:[P4VP<sub>146</sub>-TTC]<sub>0</sub>:[AIBN]<sub>0</sub> = 1800:3:3:2, the onset micellization of PNIPAM-*b*-PS and P4VP-*b*-PS occurs at 12.4% monomer conversion with the theoretical  $D_P$  of the PS block approaching to 37. (Note: the theoretical  $D_P$  were calculated according to ref 73 by approximately assuming the same  $D_P$  in PNIPAM-*b*-PS and P4VP-*b*-PS.) Because of the relatively short PS block, the organic solvent of the polymerization medium, and the relatively high polymerization temperature of 70 °C, the block copolymer micelles formed in the initial RAFT polymerization are not frozen, which ensures fast micelle exchange dynamics to form mixed micelles and ultimately formation of mixed nanoparticles constructed with the two diblock copolymers of PNIPAM-*b*-PS and P4VP-*b*-PS, as shown in Scheme 1.

The mixed nanoparticles as shown in Scheme 1 are expected to have a PNIPAM/P4VP mixed corona and a PS core. To check the structure of the mixed corona–core nanoparticles and to form MCBNs, these mixed corona–core nanoparticles dispersed in the polymerization medium of the 80/20 ethanol/

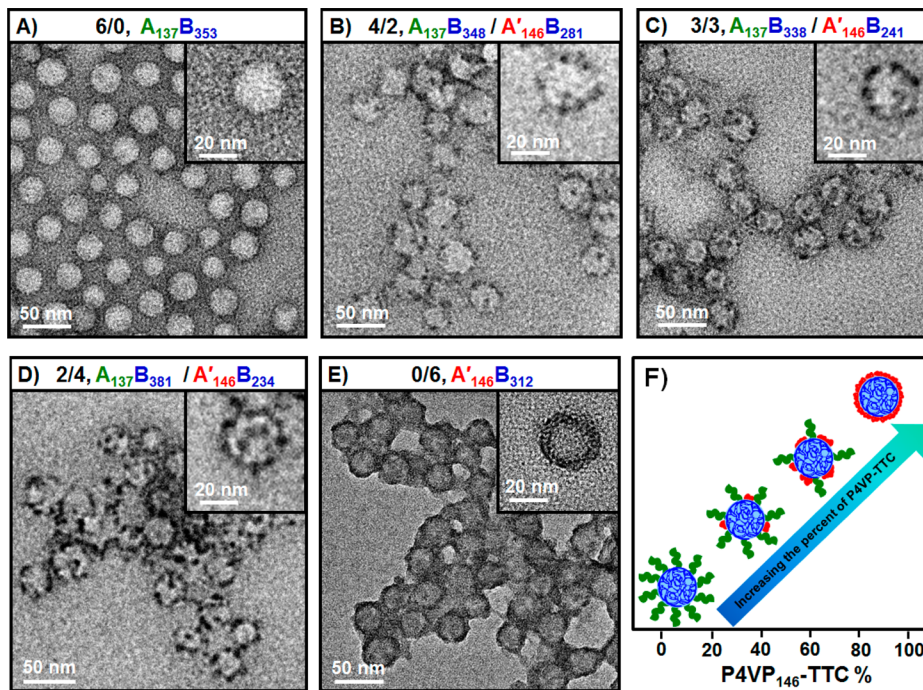


**Figure 7.** TEM images of MCBNs prepared through the two macro-RAFT agents comediated dispersion polymerization with the molar ratio of PNIPAM<sub>137</sub>-TTC/P4VP<sub>146</sub>-TTC at 6/0 (A), 4/2 (B), 3/3 (C), 2/4 (D), and 0/6 (E) and summary of the MCBNs prepared under different percent of the P4VP<sub>146</sub>-TTC macro-RAFT agent (F). Polymerization conditions: St (0.500 g, 4.80 mmol), [St]<sub>0</sub>:[PNIPAM<sub>137</sub>-TTC + P4VP<sub>146</sub>-TTC]<sub>0</sub>: [AIBN]<sub>0</sub> = 1800:6:2, the ethanol/water mixture (4.00 g, 80/20 by weight), 70 °C, 14 h.

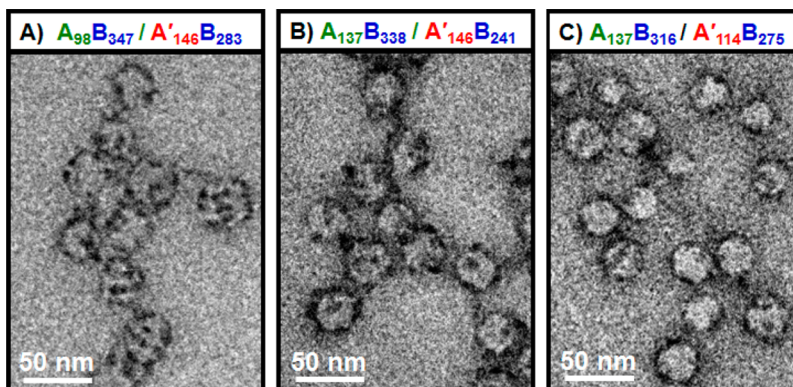


**Figure 8.** TEM images of MCBNs through the dispersion RAFT polymerization comediatorated with the two-macro-RAFT agents of PNIPAM<sub>98</sub>-TTC/P4VP<sub>146</sub>-TTC (A), PNIPAM<sub>137</sub>-TTC/P4VP<sub>146</sub>-TTC (B), and PNIPAM<sub>137</sub>-TTC/P4VP<sub>114</sub>-TTC (C). Polymerization conditions: St (0.500 g, 4.80 mmol), [St]<sub>0</sub>:[PNIPAM-TTC]<sub>0</sub>:[P4VP-TTC]<sub>0</sub>:[AIBN]<sub>0</sub> = 1800:3:3:2, the ethanol/water mixture (4.00 g, 80/20 by weight), 70 °C, 14 h.

water mixture were transferred into water. In water, the P4VP block is insoluble and deposits on the PS core whereas the PNIPAM block keeps soluble at room temperature, and therefore the mixed corona–core nanoparticles converted into MCBNs containing a PS core, discrete P4VP nodules on the PS core, and a solvophilic PNIPAM corona. The formation of discrete P4VP nodules but not an uninterrupted shell on the PS core is due to the P4VP chains being segregated by the neighboring PNIPAM chains during the P4VP deposition. To discern the P4VP, PS, and PNIPAM phases in MCBNs, MCBNs were stained jointly with phosphotungstic acid and I<sub>2</sub> vapor as discussed elsewhere<sup>10,74,75</sup> and then checked by TEM. Note: this jointed staining initially with phosphotungstic acid and then with I<sub>2</sub> helps to clearly discern the P4VP phase on the block copolymer nanoparticles. Figures 1A and 1B show the TEM images of such typical MCBNs, in which the light gray

region is ascribed to the PS core and the dark domain is due to the I<sub>2</sub>-stained P4VP nodules, whereas the solvophilic corona of the PNIPAM block is invisible. Therefore, formation of MCBNs containing a PS core with the average diameter at 28.1 nm, 4.6 nm discrete P4VP nodules on the PS core, and a PNIPAM corona as shown in Figure 1C is sufficiently concluded.

With the encouraging synthesis of well-defined MCBNs through the two macro-RAFT agents comediated dispersion polymerization, the polymerization kinetics, the evolution of MCBNs with the increasing monomer conversion, the exact composition of PNIPAM-*b*-PS and P4VP-*b*-PS in MCBNs, and the temperature and pH response of MCBNs are discussed subsequently.

### 3.3. Polymerization Kinetics and Evolution of MCBNs during the Dispersion RAFT Polymerization.

The two

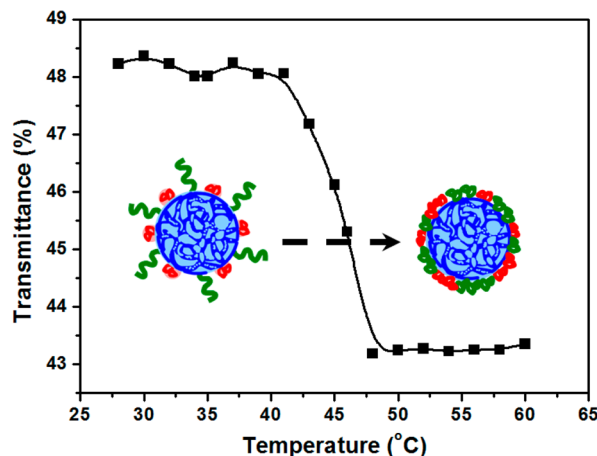


**Figure 9.** Temperature-dependent transmittance of the 0.015 wt % aqueous dispersion of the MCBNs of PNIPAM<sub>137</sub>-*b*-PS<sub>338</sub>/P4VP<sub>146</sub>-*b*-PS<sub>241</sub>. Insets: schematic morphology transition of MCBNs by temperature stimulus.

macro-RAFT agents comediated dispersion polymerization under  $[St]_0$ :[PNIPAM<sub>137</sub>-TTC]<sub>0</sub>:[P4VP<sub>146</sub>-TTC]<sub>0</sub>:[AIBN]<sub>0</sub> = 1800:3:3:2 undergoes an initial 4 h homogeneous stage as indicated by the transparent solution, micellization of the *in situ* synthesized diblock copolymers at 4 h as indicated by the bluish dispersion, and last formation of block copolymer nano-objects at the end of polymerization. There is an existing initial homogeneous stage in the dispersion RAFT polymerization is due to the synthesized diblock copolymers of PNIPAM-*b*-PS/P4VP-*b*-PS containing a short PS block being molecularly soluble in the polymerization medium. With the proceeding of the RAFT polymerization, the solvophobic PS block extends, and micellization of the *in situ* synthesized diblock copolymers occurs and the self-assembled diblock copolymer nano-objects grow with the increasing DP of the PS block. The kinetics of the two macro-RAFT agents comediated dispersion polymerization are summarized in Figure 2A. The monomer conversion increases with the polymerization time and finally reaches 88.6% in 24 h. The further increase in the polymerization time just leads to a very slight increase in the monomer conversion. Figure 2B shows the  $\ln([M]_0/[M])$  versus polymerization time plots, in which the gradient linear stage corresponds to the initial 4 h homogeneous polymerization and the steep linear

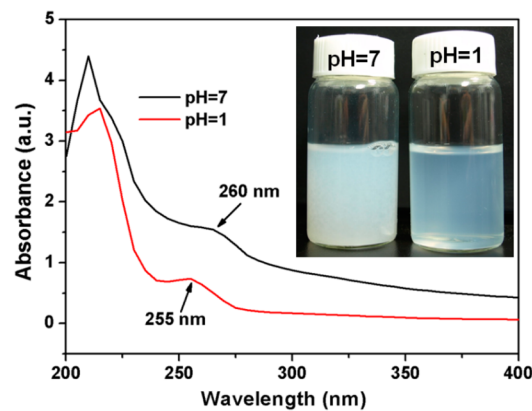


**Figure 11.** UV-vis absorption spectra of the neutral or acidic 0.5 wt % aqueous dispersion of the MCBNs of PNIPAM<sub>137</sub>-*b*-PS<sub>338</sub>/P4VP<sub>146</sub>-*b*-PS<sub>241</sub> at 25 °C. Insets: the samples of the aqueous dispersion of MCBNs.

one corresponds to the later heterogeneous polymerization. Clearly, the two macro-RAFT agents comediated dispersion polymerization undergoes a polymerization kinetics similarly with those in the individual macro-RAFT agent mediated dispersion polymerization shown in Figure S3.

Clearly, the two macro-RAFT agents comediated dispersion polymerization affords the PNIPAM-*b*-PS/P4VP-*b*-PS mixture. For brevity, PNIPAM-*b*-PS and P4VP-*b*-PS are named as AB and A'B, in which A represents the PNIPAM block, A' represents the P4VP block, and B represents the PS block in the following discussion. Interestingly, as shown in Figure 2C monomodal GPC traces at most cases of polymerization time are observed, suggesting that PNIPAM-*b*-PS and P4VP-*b*-PS in the AB/A'B mixture have similar polymer weight. Based on the GPC traces, the average molecular weight  $\bar{M}_{n, GPC}$  and PDI of the AB/A'B mixture synthesized at different polymerization time are obtained, and the results are summarized in Figure 2D. It is found that  $\bar{M}_{n, GPC}$  of the AB/A'B mixture increases linearly with the monomer conversion, and the PDI value of the AB/A'B mixture is generally below 1.3. This primary analysis affords us two conclusions. First, PNIPAM-*b*-PS and P4VP-*b*-PS in the AB/A'B mixture have similar polymer weights, and the polymer weight of the diblock copolymers should increase with the increasing monomer conversion. Second, the PDI of PNIPAM-*b*-PS and P4VP-*b*-PS should be satisfactorily low.

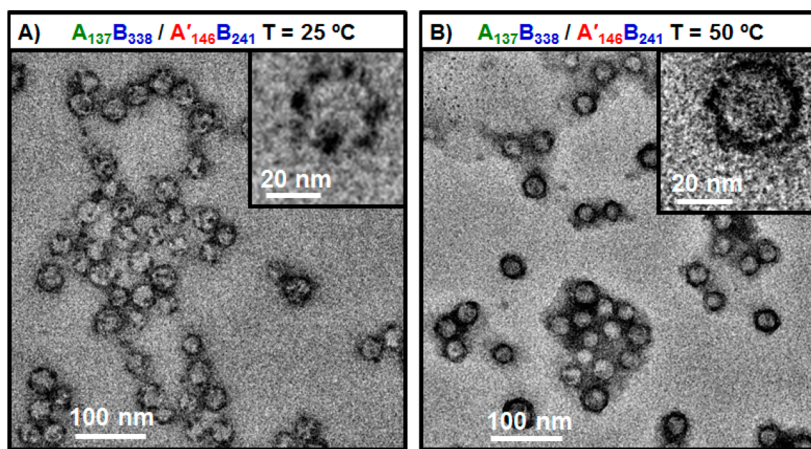


**Figure 10.** TEM images of the MCBNs of PNIPAM<sub>137</sub>-*b*-PS<sub>338</sub>/P4VP<sub>146</sub>-*b*-PS<sub>241</sub> dispersed in water at 25 °C (A) and 50 °C (B).

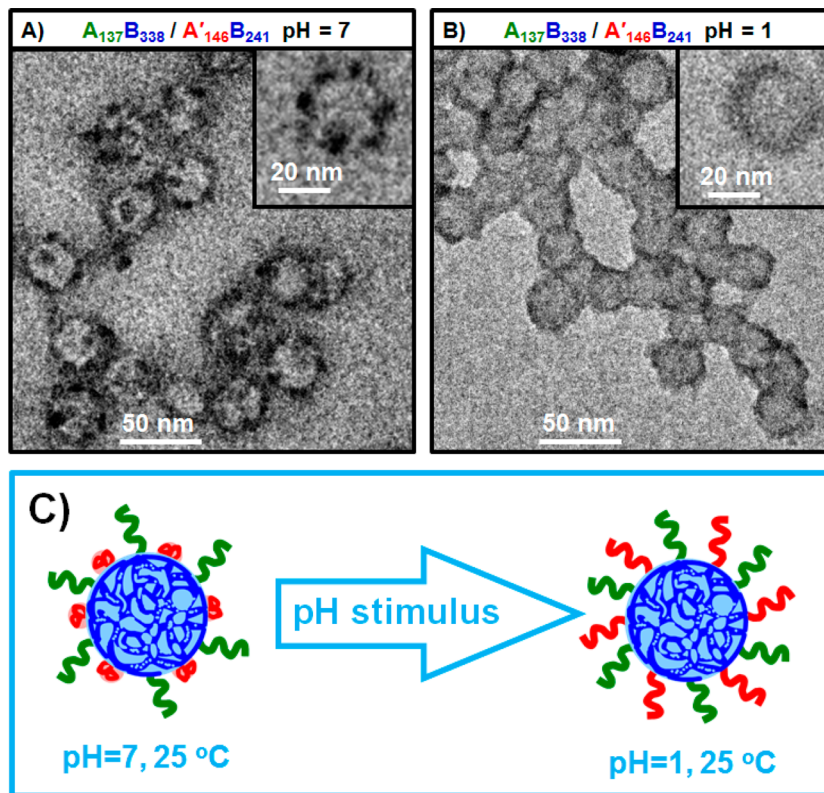


**Figure 12.** TEM images of the MCBNs of PNIPAM<sub>137</sub>-*b*-PS<sub>338</sub>/P4VP<sub>146</sub>-*b*-PS<sub>241</sub> dispersed in water at 25 °C at pH = 7 (A) and pH = 1 (B) and the schematic pH response of MCBNs (C).

To detect the exact composition of PNIPAM-*b*-PS and P4VP-*b*-PS in the AB/A'B mixture, separation of individual diblock copolymer from the AB/A'B mixture is performed. Since PNIPAM-*b*-PS is soluble in acetone (note: PNIPAM-*b*-PS becomes less soluble with the increasing DP of the PS block) and P4VP-*b*-PS is insoluble in acetone, successful separation as shown in the Experimental Section can be achieved, which is confirmed by the <sup>1</sup>H NMR spectra of the AB/A'B mixture and the separated PNIPAM-*b*-PS and P4VP-*b*-PS diblock copolymers shown in Figure 3 and Figure S4 (note: P4VP-*b*-PS was successfully separated; in the separated PNIPAM-*b*-PS, less than 5 wt % of P4VP-*b*-PS was immersed). Based on the <sup>1</sup>H NMR spectra of the AB/A'B mixture before and after separation, the molar ratio of P4VP-*b*-PS/PNIPAM-*b*-PS in the AB/A'B mixture and the molecular weight  $M_{n,NMR}$  of PNIPAM-*b*-PS and P4VP-*b*-PS can be determined. It is found that the molar ratio of PNIPAM-*b*-PS/P4VP-*b*-PS in the AB/A'B diblock copolymer mixture, 1.06, is very close to that of the fed macro-RAFT agents of P4VP<sub>146</sub>-TTC/PNIPAM<sub>137</sub>-TTC at 1, suggesting almost all the macro-RAFT agents are block-extended to form the corresponding diblock copolymers. As shown in Figure 2D, the  $M_{n,NMR}$  values of the separated PNIPAM-*b*-PS and P4VP-*b*-PS increase linearly with the monomer conversion just similarly with that in the individual macro-RAFT agent mediated dispersion polymerization.<sup>64–70</sup> The PNIPAM-*b*-PS diblock copolymer synthesized at a given monomer conversion has a slightly higher molecular weight than P4VP-*b*-PS, since the PNIPAM<sub>137</sub>-TTC macro-RAFT agent mediated RAFT polymerization runs slightly faster than that at case of P4VP<sub>146</sub>-TTC (Figure S3). Figure 4 shows the GPC traces of the typical AB/A'B mixture synthesized at the polymerization time of 16 h and the separated diblock

copolymers of PNIPAM-*b*-PS and P4VP-*b*-PS, from which the average molecular weight  $\bar{M}_{n,GPC}$  of the AB/A'B mixture and the separated diblock copolymers and the PDI values are obtained and indicated by the insets. It is found that the separated PNIPAM-*b*-PS and P4VP-*b*-PS have similar  $M_{n,GPC}$ , and the PDI, 1.1–1.2, is lower than that of the AB/A'B diblock copolymer mixture just as expected.

Figure 5 shows the TEM images of the MCBNs dispersed in water prepared through the two macro-RAFT agents comediated dispersion polymerization at different polymerization time, from which uniform MCBNs containing a PS core, several discrete P4VP nodules on the PS core, and a soluble PNIPAM corona as indicated by the insets are clearly discerned. The molar ratio of P4VP-*b*-PS/PNIPAM-*b*-PS in MCBNs is close to 1, and the detailed composition of the P4VP-*b*-PS and PNIPAM-*b*-PS diblock copolymers as indicated by the insets is shown in Figure 5. By statistical analysis of above 100 MCBNs, the average diameter of the PS core ( $D_{core}$ ) and the P4VP nodules ( $D_{nodule}$ ) in MCBNs prepared at different polymerization time are obtained, and the results are summarized in Figure 6. It is found that, with the increasing monomer conversion,  $D_{core}$  increases from 16.7 to 28.8 nm, whereas  $D_{nodule}$  decreases from 5.4 to 3.0 nm. Note: some of the P4VP nodules seem to be joined together, and therefore a very approximate estimation of  $D_{nodule}$  is made. The increasing  $D_{core}$  of the PS core with the increasing monomer conversion should be ascribed to the increasing DP of the PS block in P4VP-*b*-PS and PNIPAM-*b*-PS. The decreasing  $D_{nodule}$  of the P4VP nodules on the PS core with the increasing monomer conversion is ascribed to the increasing surface area of the PS core. The P4VP chains on the large-sized PS core are not as

crowded as those on small-sized one, and therefore they tend to form small P4VP nodules when they deposit on the PS core.

**3.4. Tuning the Structure of MCBNs.** The above-mentioned clearly shows the successful preparation of MCBNs and also indicates that the structure of MCBNs changes with the increasing DP of the PS block in the two diblock copolymers. In this section, two other methods to tune the size of the P4VP nodules on the PS core by (1) changing the percent of the P4VP-TTC macro-RAFT agent in the two macro-RAFT agents and (2) changing DP of the P4VP-TTC macro-RAFT agent are introduced. In the first method, the two macro-RAFT agents comediated dispersion polymerization was performed under  $[St]_0:[\text{PNIPAM}_{137}\text{-TTC} + \text{P4VP}_{146}\text{-TTC}]_0:[\text{AIBN}]_0 = 1800:6:2$  with different molar ratio of  $\text{PNIPAM}_{137}\text{-TTC}/\text{P4VP}_{146}\text{-TTC}$ . When the polymerization was quenched at the constant polymerization time of 14 h at monomer conversion at 80–83%, MCBNs dispersed in water at room temperature were checked by TEM (Figure 7), and the PNIPAM-*b*-PS and P4VP-*b*-PS diblock copolymers in MCBNs were separated and characterized (seeing results in the insets in Figure 7). As shown by the TEM images in Figure 7, when the molar ratio of  $\text{PNIPAM}_{137}\text{-TTC}/\text{P4VP}_{146}\text{-TTC}$  decreases from 6/0 to 4/2, to 3/3, to 2/4, and finally to 0/6 (note: in the first and last cases of 6/0 and 0/6, the dispersion RAFT polymerization mediated with the individual macro-RAFT agent of PNIPAM<sub>137</sub>-TTC or P4VP<sub>146</sub>-TTC was performed), corona–core nanoparticles of PNIPAM<sub>137</sub>-*b*-PS<sub>353</sub> (Figure 7A, in which the light gray region is ascribed to the PS core and the corona-forming PNIPAM block is invisible), MCBNs of the AB/A'B mixture (Figures 7B–D), and shell–core nanoparticles of P4VP<sub>146</sub>-*b*-PS<sub>312</sub> (Figure 7E, in which the light gray region is ascribed to the PS core and the outer dark domain is due to the I<sub>2</sub>-stained P4VP shell) are formed. It is found that all these nanoparticles including the PNIPAM<sub>137</sub>-*b*-PS<sub>353</sub> corona–core nanoparticles, MCBNs, and the P4VP<sub>146</sub>-*b*-PS<sub>312</sub> shell–core nanoparticles have a PS core with similar size at 26–28 nm. However, by checking the P4VP nodules on MCBNs, it is found that the average diameter  $D_{\text{nodule}}$  of the P4VP nodules on the PS core increases from 3.2 nm (Figure 7B) to 4.1 nm (Figure 7C) and further to 4.6 nm (Figure 7D), and finally P4VP forms a 4.7 nm shell on the PS core (Figure 7E), when the molar ratio of  $\text{PNIPAM}_{137}\text{-TTC}/\text{P4VP}_{146}\text{-TTC}$  decreases from 4/2 to 0/6. The morphology evolution of the P4VP phase on the PS core with the increasing percent of the P4VP<sub>146</sub>-TTC macro-RAFT agent is schematically summarized in Figure 7E, and the reason can be ascribed to the increasing amount of the P4VP chains on the PS core of MCBNs. In the case of low amount of the P4VP chains, the P4VP chains deposit on the PS core to form discrete P4VP nodules; with the increasing amount of the P4VP chains, the P4VP nodules become larger or are linked together to form a shell layer on the PS core.

Figure 8 shows the TEM images of the MCBNs prepared through the two macro-RAFT agents comediated dispersion polymerization under  $[St]_0:[\text{PNIPAM-TTC}]_0:[\text{P4VP-TTC}]_0:[\text{AIBN}]_0 = 1800:3:3:2$  by changing DP of the P4VP-TTC and PNIPAM-TTC macro-RAFT agents. As shown by the TEM images in Figure 8, at all the three cases of two macro-RAFT agents, PNIPAM<sub>98</sub>-TTC/P4VP<sub>146</sub>-TTC, PNIPAM<sub>137</sub>-TTC/P4VP<sub>146</sub>-TTC, and PNIPAM<sub>137</sub>-TTC/P4VP<sub>114</sub>-TTC, well-defined MCBNs have been prepared. The  $D_{\text{core}}$  of the PS core in three MCBNs at 26–28 nm is similar, whereas the average diameter  $D_{\text{core}}$  of the P4VP nodules, 4.4 nm in the case of PNIPAM<sub>98</sub>-TTC/P4VP<sub>146</sub>-TTC (Figure 8A), 4.1 nm in the

case of PNIPAM<sub>137</sub>-TTC/P4VP<sub>146</sub>-TTC (Figure 8B), and 3.5 nm in the case of PNIPAM<sub>137</sub>-TTC/P4VP<sub>114</sub>-TTC (Figure 8C) is slightly different. This suggests that the size of the P4VP nodules is possibly correlative to the DP of the P4VP-TTC macro-RAFT agent, although the effect is not as obvious as those of the P4VP<sub>146</sub>-TTC percent discussed above. The selection of the PNIPAM-TTC/P4VP-TTC macro-RAFT agents with great difference in DP is not tried, since it will lead to different onset micellization of PNIPAM-*b*-PS and P4VP-*b*-PS in the two macro-RAFT agents comediated dispersion polymerization and therefore possibly lead to nonergodic micelles constructed with one block copolymer.

### 3.5. Temperature and pH Response of MCBNs.

PNIPAM is a typical thermoresponsive polymer, which is soluble in water below the lower critical solution temperature (LCST) around 32 °C and becomes insoluble when temperature increases above LCST.<sup>76</sup> P4VP is a typical pH-responsive polymer, which is soluble in water with pH < 5 and becomes insoluble with pH > 5.<sup>77</sup> The present MCBNs constructed with the PNIPAM-*b*-PS/P4VP-*b*-PS diblock copolymers contain the thermoresponsive PNIPAM block and the pH-responsive P4VP block, and therefore their temperature and pH response are expected.

From the temperature-dependent transmittance of the aqueous dispersion of the MCBNs of P4VP<sub>146</sub>-*b*-PS<sub>241</sub>/PNIPAM<sub>137</sub>-*b*-PS<sub>338</sub> shown in Figure 9, the phase transition of the PNIPAM block in MCBNs occurs at 45 °C. Compared with the LCST of PNIPAM<sub>137</sub>-TTC (Figure S5), the phase-transition temperature (PTT) of the PNIPAM block in MCBNs is rather higher (45 °C vs 30 °C). The reason for the increasing PTT of the PNIPAM block is possibly due to the steric repulsion among the crowded PNIPAM chains tethered on the PS core of MCBNs, which retards the soluble-to-insoluble transition of PNIPAM as discussed elsewhere.<sup>78</sup> Figures 10A and 10B show the TEM images of the MCBNs dispersed in water at 25 °C below PTT and at 50 °C above PTT, from which MCBNs (Figure 10A) and shell–core nanoparticles (Figure 10B) are observed. The size of the PS core in MCBNs and the shell–core nanoparticles is almost the same at 27 nm, whereas discrete 4.1 nm P4VP nodules in MCBNs and the shell layer with the average shell thickness at 4.6 nm in the shell–core nanoparticles are observed. The transition of MCBNs to shell–core nanoparticles is possible due to the deposition of the PNIPAM chains on the PS core to make a PNIPAM/P4VP mixed shell as shown by the inset shown in Figure 9. Based on the chemical composition of the two diblock copolymers and their molar ratio and their molar ratio in the MCBNs of PNIPAM<sub>137</sub>-*b*-PS<sub>338</sub>/P4VP<sub>146</sub>-*b*-PS<sub>241</sub>, the thickness of the PNIPAM/P4VP mixed shell of the shell–core nanoparticles, 3.9 nm, is approximately calculated. Clearly, the calculated shell thickness of the shell–core nanoparticles is close to those determined by TEM, confirming our speculation. The thermoresponse of the MCBNs of P4VP<sub>146</sub>-*b*-PS<sub>241</sub>/PNIPAM<sub>137</sub>-*b*-PS<sub>338</sub> is also confirmed by DLS analysis (Figure S6), from which the shrinking  $D_h^{\text{app}}$  of MCBNs from 59 to 47 nm when temperature stepping across PTT is detected.

The pH response of the MCBNs of PNIPAM<sub>137</sub>-*b*-PS<sub>338</sub>/P4VP<sub>146</sub>-*b*-PS<sub>241</sub> is checked by the UV–vis absorption spectra of the MCBNs dispersed in acidic water (pH = 1) and in neutral water (pH = 7). As shown in Figure 11, when the aqueous dispersion of MCBNs was acidified, two changes in the spectra including (1) the decreasing absorbance and (2) the characteristic character absorption at 260 nm shifting to 255

nm were observed, confirming the pH response of MCBNs through protonation of the pyridyl group in the P4VP block. In the pH = 1 acidic solution, the pyridyl groups in the P4VP block are protonated, the P4VP block becomes soluble, and therefore the P4VP nodules on the PS core are dissolved in the acidic solvent, and the MCBNs convert into mixed corona–core nanoparticles, in which the PNIPAM block and the acidified P4VP block form the mixed corona and the PS block forms the core. This hypothesis is confirmed by DLS analysis (Figure S7) and by the TEM images of the MCBNs dispersed in water before and after acidification at 25 °C, in which MCBNs (Figure 12A) and corona–core nanoparticles (Figure 12B) are observed, respectively, and therefore the pH response of MCBNs as schematically shown in Figure 12C is concluded.

#### 4. CONCLUSIONS

Multicompartment block copolymer nanoparticles (MCBNs) arouse great interest due to their special structure and potential application. In this contribution, a new and efficient strategy to prepare well-defined MCBNs constructed with two diblock copolymers of PNIPAM-*b*-PS/P4VP-*b*-PS through the two macro-RAFT agents comediated dispersion polymerization is proposed. In this two macro-RAFT agents comediated dispersion polymerization, two diblock copolymers of PNIPAM-*b*-PS/P4VP-*b*-PS are simultaneously formed. By choosing two macro-RAFT agents of P4VP-TTC and PNIPAM-TTC with similar DP, the onset micellization of PNIPAM-*b*-PS and P4VP-*b*-PS occurs simultaneously, when the PS block extends to a critical point in the dispersion RAFT polymerization. This simultaneous micellization of PNIPAM-*b*-PS and P4VP-*b*-PS leads to mixed corona–core nanoparticles containing a PNIPAM/P4VP mixed corona and a PS core. In neutral water at room temperature, the P4VP chains of the mixed corona–core nanoparticles become insoluble and deposit on the PS core to form discrete P4VP nodules, and therefore the mixed corona–core nanoparticles convert into MCBNs containing a solvophobic PS core, discrete P4VP nodules on the PS core, and a solvophilic PNIPAM corona. The parameters affecting the structure of MCBNs are investigated. It is found that the higher percent of the P4VP-TTC macro-RAFT agent in the mixture of the two macro-RAFT agents and the shorter PS block, the larger the size of the P4VP nodules on MCBNs. The MCBNs constructed with the PNIPAM-*b*-PS/P4VP-*b*-PS diblock copolymers are temperature- and pH-responsive. Through the phase transition of the temperature-responsive PNIPAM block and the pH-responsive P4VP block, the morphology of MCBNs is changed. Our strategy of the two macro-RAFT agents comediated dispersion polymerization overcomes the inconvenience and difficulty in synthesis of MCBNs, and it provides a valid way to prepare well-defined MCBNs constructed with two or more than two diblock copolymers, which is still ongoing in our lab.

#### ■ ASSOCIATED CONTENT

##### Supporting Information

Figures S1 and S2 showing the GPC traces and the <sup>1</sup>H NMR spectra of P4VP-TTC and PNIPAM-TTC; Figure S3 showing the polymerization kinetics for the individual macro-RAFT agent mediated dispersion polymerization; Figure S4 showing the <sup>1</sup>H NMR spectra of the AB/A'B diblock copolymer mixture before and after separation and Figure S5 showing the temperature-dependent transmittance of the PNIPAM<sub>137</sub>-TTC aqueous solution; Figures S6 and S7 showing the  $D_h^{\text{app}}$

of the MCBNs of PNIPAM<sub>137</sub>-*b*-PS<sub>338</sub>/P4VP<sub>146</sub>-*b*-PS<sub>241</sub>. This material is available free of charge via the Internet at <http://pubs.acs.org>.

#### ■ AUTHOR INFORMATION

##### Corresponding Author

\*E-mail: wqzhang@nankai.edu.cn; Tel +86-22-23509794; Fax +86-22-23503510 (W.Z.).

##### Notes

The authors declare no competing financial interest.

#### ■ ACKNOWLEDGMENTS

The financial support by National Science Foundation of China (No. 21274066 and 21474054) and PCSIRT (IRT1257) is gratefully acknowledged.

#### ■ REFERENCES

- (1) Lutz, J.-F.; Laschewsky, A. *Macromol. Chem. Phys.* **2005**, *206*, 813–817.
- (2) Armado, E.; Kressler, J. *Soft Matter* **2011**, *7*, 7144–7149.
- (3) Moughtom, A. O.; Hillmyer, M. A.; Lodge, T. P. *Macromolecules* **2012**, *45*, 2–19.
- (4) Lodge, T. P.; Rasdal, A.; Li, Z.; Hillmyer, M. A. *J. Am. Chem. Soc.* **2005**, *127*, 17608–17609.
- (5) Jiang, T.; Wang, L.; Lin, S.; Lin, J.; Li, Y. *Langmuir* **2011**, *27*, 6440–6448.
- (6) Uchman, M.; Štěpánek, M.; Procházka, K. *Macromolecules* **2009**, *42*, 5605–5613.
- (7) Kyerematen, S. O.; Busse, K.; Kohlbrecher, J.; Kressler, J. *Macromolecules* **2011**, *44*, 583–593.
- (8) Sugihara, S.; Kanaoka, S.; Aoshima, S. *J. Polym. Sci., Part A: Polym. Chem.* **2004**, *42*, 2601–2611.
- (9) Weberskirch, R.; Preuschen, J.; Spiess, H. W.; Nuyken, O. *Macromol. Chem. Phys.* **2000**, *201*, 995–1007.
- (10) Huo, F.; Li, S.; Li, Q.; Qu, Y.; Zhang, W. *Macromolecules* **2014**, *47*, 2340–2349.
- (11) Cao, Y.; Zhao, N.; Wu, K.; Zhu, X. X. *Langmuir* **2009**, *25*, 1699–1704.
- (12) Kubowicz, S.; Baussard, J.-F.; Lutz, J.-F.; Thünemann, A. F.; Berlepsch, H. v.; Laschewsky, A. *Angew. Chem., Int. Ed.* **2005**, *44*, 5262–5265.
- (13) Berlepsch, H. v.; Böttcher, C.; Skrabania, K.; Laschewsky, A. *Chem. Commun.* **2009**, *17*, 2290–2292.
- (14) Marsat, J.-N.; Heydenreich, M.; Kleinpeter, E.; Berlepsch, H. v.; Böttcher, C.; Laschewsky, A. *Macromolecules* **2011**, *44*, 2092–2105.
- (15) Cui, H.; Chen, Z.; Zhong, S.; Wooley, K. L.; Pochan, D. J. *Science* **2007**, *317*, 647–650.
- (16) Sun, G.; Cui, H.; Lin, L. Y.; Lee, N. S.; Yang, C.; Neumann, W. L.; Freskos, J. N.; Shieh, J. J.; Dorshow, R. B.; Wooley, K. L. *J. Am. Chem. Soc.* **2011**, *133*, 8534–8543.
- (17) Chen, Z.; Cui, H.; Hales, K.; Li, Z.; Qi, K.; Pochan, D. J.; Wooley, K. L. *J. Am. Chem. Soc.* **2005**, *127*, 8592–8593.
- (18) Pochan, D. J.; Chen, Z.; Cui, H.; Hales, K.; Qi, K.; Wooley, K. L. *Science* **2004**, *306*, 94–97.
- (19) Dupont, J.; Liu, G. *Soft Matter* **2010**, *6*, 3654–3661.
- (20) Gao, Y.; Li, X.; Hong, L.; Liu, G. *Macromolecules* **2012**, *45*, 1321–1330.
- (21) Fang, B.; Walther, A.; Wolf, A.; Xu, Y.; Yuan, J.; Müller, A. H. E. *Angew. Chem., Int. Ed.* **2009**, *48*, 2877–2880.
- (22) Schacher, F.; Walther, A.; Ruppel, M.; Drechsler, M.; Müller, A. H. E. *Macromolecules* **2009**, *42*, 3540–3548.
- (23) Gröschel, A. H.; Schacher, F. H.; Schmalz, H.; Borisov, O. V.; Zhulina, E. B.; Walther, A.; Müller, A. H. E. *Nat. Commun.* **2012**, *3*, 1–10.
- (24) Gröschel, A. H.; Walther, A.; Löbling, T. I.; Schmelz, J.; Hanisch, A.; Schmalz, H.; Müller, A. H. E. *J. Am. Chem. Soc.* **2012**, *134*, 13850–13860.

- (25) Gröschel, A. H.; Walther, A.; Löbling, T. I.; Schacher, F. H.; Schmalz, H.; Müller, A. H. E. *Nature* **2013**, *503*, 247–251.
- (26) Hanisch, A.; Gröschel, A. H.; Förtsch, M.; Drechsler, M.; Jinnai, H.; Ruhland, T. M.; Schacher, F. H.; Müller, A. H. E. *ACS Nano* **2013**, *7*, 4030–4041.
- (27) Saito, N.; Liu, C.; Lodge, T. P.; Hillmyer, M. A. *ACS Nano* **2010**, *4*, 1907–1912.
- (28) Li, Z.; Kesselman, E.; Talmon, Y.; Hillmyer, M. A.; Lodge, T. P. *Science* **2004**, *306*, 98–101.
- (29) Li, Z.; Hillmyer, M. A.; Lodge, T. P. *Langmuir* **2006**, *22*, 9409–9417.
- (30) Liu, C.; Hillmyer, M. A.; Lodge, T. P. *Langmuir* **2008**, *24*, 12001–12009.
- (31) Saito, N.; Liu, C.; Lodge, T. P.; Hillmyer, M. A. *Macromolecules* **2008**, *41*, 8815–8822.
- (32) Wang, L.; Xu, R.; Wang, Z.; He, X. *Soft Matter* **2012**, *8*, 11462–11470.
- (33) Ge, Z.; Liu, S. *Macromol. Rapid Commun.* **2009**, *30*, 1523–1532.
- (34) Zhang, Y.; Liu, H.; Dong, H.; Li, C.; Liu, S. *J. Polym. Sci., Part A: Polym. Chem.* **2009**, *47*, 1636–1650.
- (35) Mao, J.; Ni, P.; Mai, Y.; Yan, D. *Langmuir* **2007**, *23*, 5127–5134.
- (36) Brannan, A. K.; Bates, F. S. *Macromolecules* **2004**, *37*, 8816–8819.
- (37) Thünemann, A. F.; Kubowicz, S.; von Berlepsch, H.; Möhwald, H. *Langmuir* **2006**, *22*, 2506–2510.
- (38) Tsitsilianis, C.; Stavrouli, N.; Bocharova, V.; Angelopoulos, S.; Kiriy, A.; Katsampas, I.; Stamm, M. *Polymer* **2008**, *49*, 2996–3006.
- (39) Gohy, J.-F.; Ott, C.; Hoeppener, S.; Schubert, U. S. *Chem. Commun.* **2009**, *9*, 6038–6040.
- (40) Hoogenboom, R.; Wiesbrock, F.; Leenen, M. A. M.; Thijs, H. M. L.; Huang, H.; Fustin, C.-A.; Guillet, P.; Gohy, J.-F.; Schubert, U. S. *Macromolecules* **2007**, *40*, 2837–2843.
- (41) Schacher, F.; Betthausen, E.; Walther, A.; Schmalz, H.; Pergushov, D. V.; Müller, A. H. E. *ACS Nano* **2009**, *3*, 2095–2102.
- (42) Zhu, J.; Hayward, R. C. *Macromolecules* **2008**, *41*, 7794–7797.
- (43) Price, E. W.; Guo, Y.; Wang, C. W.; Moffitt, M. G. *Langmuir* **2009**, *25*, 6398–6406.
- (44) Christian, D. A.; Tian, A.; Ellenbroek, W. G.; Levental, I.; Rajagopal, K.; Janmey, P. A.; Liu, A. J.; Baumgart, T.; Discher, D. E. *Nat. Mater.* **2009**, *8*, 843–849.
- (45) Gohy, J.-F.; Lefevre, N.; D'Haese, C.; Hoeppener, S.; Schubert, U. S.; Kostov, G.; Ameduri, B. *Polym. Chem.* **2011**, *2*, 328–332.
- (46) Li, Z.; Hillmyer, M. A.; Lodge, T. P. *Macromolecules* **2006**, *39*, 765–771.
- (47) Pochan, D. J.; Zhu, J.; Zhang, K.; Wooley, K. L.; Miesch, C.; Emrick, T. *Soft Matter* **2011**, *7*, 2500–2506.
- (48) Zhu, J.; Zhang, S.; Zhang, K.; Wang, X.; Mays, J. W.; Wooley, K. L.; Pochan, D. J. *Nat. Commun.* **2013**, *4*, 1–7.
- (49) Zhu, J.; Zhang, S.; Zhang, F.; Wooley, K. L.; Pochan, D. J. *Adv. Funct. Mater.* **2013**, *23*, 1767–1773.
- (50) Srinivas, G.; Pitera, J. W. *Nano Lett.* **2008**, *8*, 611–618.
- (51) Zheng, R.; Liu, G.; Yan, X. *J. Am. Chem. Soc.* **2005**, *127*, 15358–15359.
- (52) Yan, X.; Liu, G.; Hu, J.; Willson, C. G. *Macromolecules* **2006**, *39*, 1906–1912.
- (53) Cheng, L.; Lin, X.; Wang, F.; Liu, B.; Zhou, J.; Li, J.; Li, W. *Macromolecules* **2013**, *46*, 8644–8648.
- (54) Liu, X.; Gao, H.; Huang, F.; Pei, X.; An, Y.; Zhang, Z.; Shi, L. *Polymer* **2013**, *54*, 3633–3640.
- (55) Yoo, S. I.; Sohn, B.-H.; Zin, W.-C.; Jung, J. C.; Park, C. *Macromolecules* **2007**, *40*, 8323–8328.
- (56) Jain, S.; Bates, F. S. *Macromolecules* **2004**, *37*, 1511–1523.
- (57) Choi, S.-H.; Lodge, T. P.; Bates, F. S. *Phys. Rev. Lett.* **2010**, *104*, 047802.
- (58) Li, S.; He, X.; Li, Q.; Shi, P.; Zhang, W. *ACS Macro Lett.* **2014**, *3*, 916–921.
- (59) Charleux, B.; Delaittre, G.; Rieger, J.; Agosto, F. D' *Macromolecules* **2012**, *45*, 6753–6765.
- (60) Sun, J.-T.; Hong, C.-Y.; Pan, C.-Y. *Soft Matter* **2012**, *8*, 7753–7767.
- (61) Lai, J. T.; Filla, D.; Shea, R. *Macromolecules* **2002**, *35*, 6754–6756.
- (62) Gao, C.; Li, Q.; Cui, Y.; Huo, F.; Li, S.; Su, Y.; Zhang, W. *J. Polym. Sci., Part A: Polym. Chem.* **2014**, *52*, 2155–2165.
- (63) Dan, M.; Huo, F.; Zhang, X.; Wang, X.; Zhang, W. *J. Polym. Sci., Part A: Polym. Chem.* **2013**, *51*, 1573–1584.
- (64) Shen, W.; Chang, Y.; Liu, G.; Wang, H.; Cao, A.; An, Z. *Macromolecules* **2011**, *44*, 2524–2530.
- (65) Zhang, W.-J.; Hong, C.-Y.; Pan, C.-Y. *Macromolecules* **2014**, *47*, 1664–1671.
- (66) Li, Y.; Armes, S. P. *Angew. Chem., Int. Ed.* **2010**, *49*, 4042–4046.
- (67) Sugihara, S.; Blanazs, A.; Armes, S. P.; Ryan, A. J.; Lewis, A. L. *J. Am. Chem. Soc.* **2011**, *133*, 15707–15713.
- (68) Pei, Y.; Lowe, A. B. *Polym. Chem.* **2014**, *5*, 2342–2351.
- (69) Xiao, X.; He, S.; Dan, M.; Huo, F.; Zhang, W. *Chem. Commun.* **2014**, *50*, 3969–3972.
- (70) Li, Q.; Gao, C.; Li, S.; Huo, F.; Zhang, W. *Polym. Chem.* **2014**, *5*, 2961–2972.
- (71) Houillot, L.; Bui, C.; Save, M.; Charleux, B. *Macromolecules* **2007**, *40*, 6500–6509.
- (72) Nicolai, T.; Colombani, O.; Chassenieux, C. *Soft Matter* **2010**, *6*, 3111–3118.
- (73) Brouwer, H. D.; Schellekens, M. A. J.; Klumperman, B.; Monteiro, M. J.; German, A. L. *J. Polym. Sci., Part A: Polym. Chem.* **2000**, *38*, 3596–3603.
- (74) Koga, T.; Kamiwatari, S.; Higashi, N. *Langmuir* **2013**, *29*, 15477–15484.
- (75) Pale, V.; Nikkonen, T.; Vapaavuori, J.; Kostainen, M.; Kavakka, J.; Selin, J.; Tittonen, I.; Helaja, J. *J. Mater. Chem. C* **2013**, *1*, 2166–2173.
- (76) Plummer, R.; Hill, D. J. T.; Whittaker, A. K. *Macromolecules* **2006**, *39*, 8379–8388.
- (77) Liu, F.; Eisenberg, A. J. *Am. Chem. Soc.* **2003**, *125*, 15059–15064.
- (78) Yang, C.; Kizhakkedathu, J. N.; Brooks, D. E.; Jin, F.; Wu, C. J. *Phys. Chem. B* **2004**, *108*, 18479–18484.